

## DISPERSION EFFECTS ON THERMAL CONVECTION IN POROUS MEDIA

Oddmund Kvernfold and

Peder A. Tyvand

Department of Mechanics

University of Oslo

### ABSTRACT

The influence of hydrodynamic dispersion on thermal convection in porous media is studied theoretically. The fluid-saturated porous layer is homogeneous, isotropic and bounded by two infinite horizontal planes kept at constant temperatures. The supercritical, steady two-dimensional motion, the heat transport and the stability of the motion are investigated. The dispersion effects depend strongly on the Rayleigh number and on the ratio of grain diameter to layer depth. The present results provide new and closer approximations to experimental data of the heat transport.

1. INTRODUCTION

The subject of this paper is buoyancy-driven convection in a fluid-saturated porous medium. Horton & Rogers (1945) showed theoretically that convection currents are possible in a porous layer heated from below. Since then, much theoretical and experimental research has been reported in this field. We refer to Combarous & Bories (1975), who also outlined important geophysical and technical applications.

A porous medium is described in terms of an average continuum representation (Bear, 1972). Local deviations from the average velocity and pressure are significant, and are accounted for, implicitly, in the macroscopic concept of permeability. Local temperature and velocity deviations give rise to the macroscopic concept of hydrodynamic dispersion. The influence of heat dispersion on porous convection is investigated in this paper.

Hydrodynamic dispersion is always present in the macroscopic description of a diffusion process taking place in a fluid flow through a porous medium. Its magnitude relative to the molecular diffusion is an increasing function of the Péclet number.

The theory of hydrodynamic dispersion was initiated by Taylor (1953) and reached an advanced level through the works by Saffman (1959,1960). Saffman's theory is complemented by Bear (1969) who used a different approach. The short, but valuable contribution by Poreh (1965) is worth mentioning.

Hydrodynamic dispersion has usually been connected with spreading of solutes and miscible displacement (Fried & Combarous, 1971). This is due to the important applications in oil production (Pfannkuch, 1963) and groundwater pollution (Fried, 1975).

Hydrodynamic dispersion may also be important in connection with buoyancy-driven convection in porous media. The onset of convection when a basic flow is present has been analyzed by Rubin (1974), Weber (1975) and Tyvand (1977). When the Péclet number is large, dispersion causes a strong delay of the onset of convection.

In finite amplitude convection without basic flow the Péclet number may become large enough for the heat dispersion to be important, even in the moderately supercritical regime of stable rolls. This is the case when the medium is relatively coarse, i.e. the ratio of layer depth to grain diameter being small. This has been pointed out in the nonlinear study by Neischloss & Dagan (1975). They solved the stationary problem to sixth order in the series expansion proposed by Kuo (1961). In the present paper this stationary problem is solved numerically. The stability of the motion is also investigated. Our main results for the heat transport sharply contradict the corresponding results by Neischloss & Dagan (1975). There is agreement at slightly supercritical Rayleigh numbers only.

Straus (1974) and Kvernold (1975) have performed similar analyses with neglect of dispersion. The present results provide improved approximations to experimental data of convective heat transfer through a horizontal porous layer heated from below.

## 2. FORMULATION OF THE MATHEMATICAL PROBLEM

A fluid saturated porous layer between two infinite horizontal planes is considered. The boundaries are impermeable and perfectly heat-conducting. The planes are separated by a distance  $h$  and have constant temperatures  $T_0$  and  $T_0 - \Delta T$ , the lower plane being the warmer. The saturated porous medium is homogeneous and isotropic. It has permeability  $K$  and molecular thermal diffusivity  $\kappa_m$ .

We choose

$$h, (c_p \rho)_m h^2 / \lambda_m, \kappa_m / h, \Delta T, \rho_0 \nu \kappa / K \quad (2.1)$$

as units of length, time  $t$ , velocity  $\vec{v} = (u, v, w)$ , temperature  $T$  and pressure  $p$ , respectively.  $c_p$  is the specific heat at constant pressure,  $\rho$  the density,  $\rho_0$  a standard density,  $\lambda_m$  the thermal conductivity of the saturated medium and  $\nu$  the kinematic viscosity of the fluid. Subscript  $m$  refers to the mixture of solid and fluid.

According to Bear (1972, p.652), the dimensionless equations may be written

$$\vec{v} + \nabla p - Ra T \vec{k} = 0 \quad (2.2)$$

$$\nabla \cdot \vec{v} = 0 \quad (2.3)$$

$$\frac{\partial T}{\partial t} + \vec{v} \cdot \nabla T = \nabla \cdot (\mathcal{D} \cdot \nabla T) \quad (2.4)$$

Here Darcy's law and the Boussinesq approximation have been applied, and the density is assumed to be a linear function of the temperature.  $\vec{k}$  is a unit vector directed opposite gravity.  $Ra$  is the Rayleigh number

$$Ra = \frac{Kg\gamma\Delta Th}{\kappa_m v} \quad (2.5)$$

where  $g$  is the gravitational acceleration and  $\gamma$  the coefficient of thermal volume expansion.  $\mathcal{D}$  is the dimensionless dispersion tensor.

Assuming that the Péclet number is less than 10, say, the dispersion tensor is with good accuracy written as

$$\mathcal{D} = (1 + \varepsilon_2 \vec{v}^2) \mathcal{E} + (\varepsilon_1 - \varepsilon_2) \vec{v} \vec{v} \quad (2.6)$$

where  $\mathcal{E}$  is the unit tensor. This tensor form has been derived by Poreh (1965) and, in a different way, by Bear (1969).  $\varepsilon_1$  and  $\varepsilon_2$  are coefficients of longitudinal and lateral dispersion, respectively, relatively to the flow direction (Weber, 1975).

The Péclet number is defined as

$$Pe = Ud/\kappa_f \quad (2.7)$$

where  $U$  is a characteristic, dimensional fluid velocity,  $\kappa_f$  the thermal diffusivity of the fluid and  $d$  is a characteristic pore length. The porous medium is assumed to be composed of grains. Then  $d$  is taken equal to the average grain diameter. It is reasonable to regard  $Pe$  as a field variable. From (2.1) and (2.7) we then find

$$Pe = |\vec{v}| \frac{\kappa_m}{\kappa_f} \frac{d}{h} \quad (2.8)$$

Saffman (1960) has determined the dispersion coefficients  $\varepsilon_1$  and  $\varepsilon_2$  theoretically :

$$\epsilon_1 = \frac{D}{15}, \quad \epsilon_2 = \frac{D}{40} \quad (2.9)$$

Here  $D$  is defined by

$$D = \frac{\kappa_m}{\kappa_f} \frac{d^2}{h^2} \quad (2.10)$$

$D$  is a dimensionless number, which will be termed "the dispersion factor".

Existing measurements cannot be regarded as acid tests on the validity of Saffman's formulae (2.9). This is due to experimental difficulties. Mechanical dispersion is measured as the difference between the two factors "effective diffusion" and "molecular diffusion". In the relevant range of Péclet numbers ( $Pe < 10$ ), the uncertainty in each of these factors is highly comparable to the mechanical dispersion itself. See, for example, the data presented by Fried & Combarous (1971)

Saffman's analysis is only concerned with the case of a solid matrix being insulating with respect to the diffusive component. The formulae (2.9) will also be assumed valid in the case of a thermally conducting matrix. This is compatible with the experiments by Green (1963). Theory is lacking at this point. But heuristic arguments with emphasis on dispersion as a mechanical mixing phenomenon may be put forward, favouring the assumption above.

A cartesian coordinate system is introduced in our model. The  $z$ -axis is directed opposite gravity, and the  $x$ - and  $y$ -axes are located at the lower boundary.  $\vec{i}$ ,  $\vec{j}$  and  $\vec{k}$  denote unit vectors in  $x$ -,  $y$ - and  $z$ -direction, respectively.

From (2.2) it follows that  $\vec{k} \cdot \nabla \times \vec{v} = 0$ , and the velocity field is solenoidal (2.3). Then the velocity is a poloidal vector

$$\vec{v} = \nabla \times (\nabla \times \vec{k} \psi) = \vec{i} \psi_{xz} + \vec{j} \psi_{yz} - \vec{k} \nabla_1^2 \psi \equiv \delta \psi \quad (2.11)$$

given by a scalar function  $\psi$ .

The temperature field is written as

$$T = T_0 / \Delta T - z + \theta(x, y, z, t) \quad (2.12)$$

By eliminating the pressure from (2.2), we obtain

$$\theta = - Ra^{-1} \nabla^2 \psi \quad (2.13)$$

By introducing (2.13) into (2.4) and utilizing (2.11), we obtain the governing equation :

$$\begin{aligned} (\nabla^4 + Ra \nabla_1^2 - \frac{\partial}{\partial t} \nabla^2) \psi &= \vec{v} \cdot \nabla \nabla^2 \psi \\ - 2 \epsilon_2 Ra \vec{v} \cdot \frac{\partial \vec{v}}{\partial z} + (\epsilon_1 - \epsilon_2) Ra \vec{v} \cdot \nabla \nabla_1^2 \psi & \\ - \epsilon_2 \vec{v}^2 \nabla^4 \psi - \epsilon_2 \nabla \vec{v}^2 \cdot \nabla \nabla^2 \psi & \\ - (\epsilon_1 - \epsilon_2) \vec{v} \cdot \nabla (\vec{v} \cdot \nabla \nabla^2 \psi) & \end{aligned} \quad (2.14)$$

The requirements of perfectly heat-conducting and impermeable boundaries lead to the boundary conditions

$$\theta = w = 0 \quad \text{at } z = 0, 1 \quad (2.15)$$

Written in terms of  $\psi$ , this is equivalent to

$$\psi = \psi_{zz} = 0 \quad \text{at } z = 0, 1 \quad (2.16)$$

Dispersion enters our problem solely through nonlinear terms, see (2.14). Therefore dispersion does not influence the onset of convection, see Neischloss & Dagan (1975). The critical Rayleigh number

for the onset of convection is

$$Ra_c = 4\pi^2 \quad (2.17)$$

corresponding to half-cell width equal to layer depth, i.e. critical wave number  $\alpha_c = \pi$ . These results were first obtained by Horton & Rogers (1945).

### 3. SOLUTION OF THE NONLINEAR EQUATIONS

We are going to study the finite amplitude motion occurring at moderately supercritical Rayleigh numbers. To obtain satisfactorily accurate solutions, it is necessary to apply numerical methods. By means of Galerkin's procedure we will find a stationary solution (2.14) and examine the stability of this solution with respect to small disturbances.

It can be shown, along the lines of Schlüter, Lortz & Busse (1965) that only two-dimensional rolls may be a stable solution of the stationary problem (2.14) for small supercritical Rayleigh numbers. This stationary two-dimensional solution subject to the boundary conditions (2.16) is formally written as an infinite series :

$$\psi = \sum_{p=-\infty}^{\infty} \sum_{q=1}^{\infty} A_{pq} e^{ip\alpha x} \sin q \pi z \quad (3.1)$$

where each term satisfies the boundary conditions. The symmetry of the problem implies the restriction

$$A_{pq} = A_{-pq} \quad (3.2)$$



corresponding to convection cells without tilt.

The expression for  $\psi$  (3.1) is substituted into (2.14). The resulting equation is multiplied by  $e^{-in\alpha x} \sin m\pi z$  and averaged over the whole fluid layer. An infinite set of algebraic equations for the unknown amplitudes  $A_{nm}$  is found :

$$G_{pqnm} A_{nm} + U_{pqnmrs} A_{nm} A_{rs} + V_{pqnmrskl} A_{nm} A_{rs} A_{kl} = 0 \quad (3.3)$$

The matrix  $G$  is a function of  $\alpha$  and  $Ra$ . The matrices  $U$  and  $V$  are functions of  $\alpha$ ,  $Ra$ , and  $D$ .

In order to solve the set (3.3) the series must be truncated. We choose to retain only terms with

$$|n| + (m+1)/2 \leq N \quad (3.4)$$

where  $N$  is a sufficiently large number, termed the truncation parameter. Due to the symmetry of the equations (3.3) the solution contains only amplitudes with  $n+m$  even, giving  $N(N+1)/2$  equations to be solved.

$Ra/Ra_c = 10, \quad \alpha/\pi = 1.8, \quad D = \frac{1}{150}$

Truncation	Nusselt number
$n + (m+1)/2 \leq 6$	6.78
$n + (m+1)/2 \leq 7$	6.81
$n + (m+3)/4 \leq 5$	6.83
$n + m \leq 10$	6.75

TABLE 1. Convergence of numerical solution indicated by values of  $Nu$  for different truncations.

With our choice of truncation computer capacity forbids us to make any careful examination with  $N$  larger than 6. This is due to the triple term in (3.3), represented by the matrix  $V$ . To test the convergence, we have compared the solutions corresponding to  $N = 6$  and  $N = 7$ . Two other truncations have also been tried. The results are given in table 1. The physical quantity concentrated upon is the Nusselt number :

$$\begin{aligned} \text{Nu} &= \frac{Qh}{\lambda_m \Delta T} = - \vec{k} \cdot (\overline{\mathcal{D}} \cdot \Delta T)_{z=0} \\ &= [1 - \overline{\theta}_z + \epsilon_2 \overline{u^2} - \epsilon_2 \overline{u^2 \theta_z}]_{z=0} \end{aligned} \quad (3.5)$$

$Q$  is the heat transport per unit time and area through the layer. The overbar denotes a horizontal average.

After having obtained a solution,  $\psi_s$ , of the stationary problem, the stability of this solution with respect to small disturbances is examined. By introducing  $\psi = \psi_s + \psi'$  into (2.14) and linearizing with respect to the infinitesimal disturbances  $\psi'$ , the following equation is found:

$$\begin{aligned} (\nabla^4 + \text{Ra} \nabla_1^2 - \frac{\partial}{\partial t} \nabla^2) \psi' &= \vec{\delta} \psi' \cdot \nabla \nabla^2 \psi_s + \vec{\delta} \psi_s \cdot \nabla \nabla^2 \psi' \\ &- 2\epsilon_2 \text{Ra} (\vec{\delta} \psi' \cdot \frac{\partial}{\partial z} \vec{\delta} \psi_s + \vec{\delta} \psi_s \cdot \frac{\partial}{\partial z} \vec{\delta} \psi') \\ &+ (\epsilon_1 - \epsilon_2) \text{Ra} (\vec{\delta} \psi' \cdot \nabla \nabla_1^2 \psi_s + \vec{\delta} \psi_s \cdot \nabla \nabla_1^2 \psi') \\ &- \epsilon_2 (2\vec{\delta} \psi' \cdot \vec{\delta} \psi_s \nabla^4 \psi_s + (\vec{\delta} \psi_s)^2 \nabla^4 \psi') - \epsilon_2 (2\nabla (\vec{\delta} \psi' \cdot \vec{\delta} \psi_s) \cdot \nabla \nabla^2 \psi_s \\ &+ \nabla (\vec{\delta} \psi_s)^2 \cdot \nabla \nabla^2 \psi') - (\epsilon_1 - \epsilon_2) [\vec{\delta} \psi' \cdot \nabla (\vec{\delta} \psi_s \cdot \nabla \nabla^2 \psi_s) \\ &+ \vec{\delta} \psi_s \cdot \nabla (\vec{\delta} \psi' \cdot \nabla \nabla^2 \psi_s) + \vec{\delta} \psi_s \cdot \nabla (\vec{\delta} \psi_s \cdot \nabla \nabla^2 \psi')] \end{aligned} \quad (3.6)$$

with boundary conditions

$$\psi' = \psi'_{zz} = 0 \quad \text{at} \quad z = 0, 1 \quad (3.7)$$

If there exists a solution of (3.6) with growing time dependence, the stationary solution is said to be unstable. Otherwise it is stable.

A general expression for the perturbation,  $\psi'$ , is given by

$$\psi' = \sum_{p,q} A_{pq} e^{ipax} e^{i(ax+by)+\sigma t} \sin q \pi z \quad (3.8)$$

where  $a$  and  $b$  are free parameters. The series (3.8) is introduced into the equation (3.6). The resulting equation is multiplied by  $e^{-inax} e^{-i(ax+by)-\sigma t} \sin n \pi z$  and averaged over the whole fluid layer. As in the stationary problem only terms with  $|n| + (m+1)/2 \leq N$  are retained. The system of linear homogeneous equations constitute an eigenvalue problem for  $\sigma$ , giving

$$\sigma = \sigma(Ra, \alpha, D, a, b) \quad (3.9)$$

The most unstable disturbances correspond to  $a = 0$  and  $b \neq 0$  as in ordinary porous convection, see Straus (1974) and Kvernfold (1975). These disturbances are termed cross-rolls if  $b$  is of the same order of magnitude as  $\alpha$ , and zig-zags if  $b$  is very small.

#### 4. DISCUSSION OF SOLUTIONS

In this chapter some characteristic features of the numerical solutions will be discussed. We first concentrate on the two-dimensional stationary problem.

The heat transport is a quantity of major physical interest. It is given by the Nusselt number defined by (3.5). In addition to the ordinary diffusion term,  $(-\bar{\theta}_z)_{z=0}$  which contains dispersion

implicitly, there are two new terms with explicit dispersion dependence. These are a term of second degree,  $(\epsilon_2 \bar{u}^2)_{z=0}$ , and one of third degree  $(-\epsilon_2 \overline{u^2 \theta})_{z=0}$ . The sum of these two terms has to be positive.

The calculations show that dispersion always reduces the average temperature gradient at the boundary. Up to  $Ra/Ra_c = 1.63$  the Nusselt number is also reduced, compared with ordinary porous convection. In table 2 some values of Nu at small supercritical Rayleigh numbers are given. The analytical result is given by the first approximation in nonlinear theory :

$$Nu = 1 + 2(Ra/Ra_c - 1)[1 + 2\pi^2(-2\epsilon_1 + \epsilon_2)] \quad (4.1)$$

Ra/Ra <sub>c</sub> \ D		D				
		0	$\frac{1}{600}$	$\frac{1}{150}$	$\frac{1}{96}$	$\frac{1}{24}$
Analytical	1.2	1.400	1.399	1.394	1.391	1.364
Numerical	1.2	1.352	1.351	1.349	1.347	1.333
-"-	1.4	1.634	1.633	1.631	1.629	1.613
-"-	1.6	1.870	1.870	1.869	1.869	1.860
-"-	1.8	2.072	2.074	2.076	2.079	2.086

TABLE 2: Analytical (formula (4.1)) and numerical results for the Nusselt number when  $\alpha = \pi$ .

which was first derived by Neischloss & Dagan (1975). It only gives the slopes at which the Nusselt number curves start out. Due to the strong curvature of these curves (see fig. 1), formula (4.1) is not a good approximation. However, it agrees qualitatively with the numerical results for small supercritical Rayleigh numbers.

The heat transport is increased by dispersion when  $Ra > 1.63 Ra_c$ .

At first this increase is very small, but it grows rapidly with the Rayleigh number. From four or five times the critical Rayleigh number, the dispersion effects on the heat transport become important. See fig. 1, where  $Nu$  is displayed as a function of  $Ra/Ra_c$  for different values of  $D$ . Here the Nusselt number has been maximized with respect to the wave number. If  $D$  is not too small, the Nusselt number curve possesses an inflexion point.

The strong increase in the Nusselt number at large Rayleigh numbers primarily arises from the third degree term. This is shown in table 3, where the contributions to the Nusselt number from the first, second and third degree terms are listed for some cases. Some approximations for these terms are also listed, disclosing the importance of solving the full problem. It is indicated that the basic contribution to the third degree term is expressed by  $(-\epsilon_2 \bar{u}^2 \bar{\theta}_z)_{z=0}$ .

There are fundamental discrepancies between our numerical results and the corresponding analytical results by Neischloss & Dagan (1975). Only at slightly supercritical Rayleigh numbers the theories agree.

In fig. 1, we choose the wave number which gives maximum Nusselt number. The variation of the Nusselt number with the wave number is exhibited in figure 2, for the case  $D = 1/80$ . Curves for  $Ra/Ra_c$  equal to 2, 4, 6, 8 and 10 are shown. For comparison the corresponding curves for  $D = 0$  are also displayed (dashed curves). Dispersion turns out to reduce the wave number of maximum heat transport considerably.

$R/R_c$	3	6	6	6
$\alpha/\pi$	1	1	1	2
D	1/60	1/60	1/100	1/100
$1 - (\bar{\theta}_z)_{z=0}$	2.775	3.588	3.810	4.099
$\epsilon_2(\overline{u^2})_{z=0}$	0.122	0.522	0.292	0.179
$-\epsilon_2(\overline{u^2\theta_z})_{z=0}$	0.203	1.215	0.739	0.520
Nu	3.100	5.325	4.841	4.798
$Nu(D=0)$	2.927	4.070	4.070	4.435
$\epsilon_2[\overline{u^2(D=0)}]_{z=0}$	0.122	0.406	0.243	0.165
$-\epsilon_2[\overline{u^2\theta_z(D=0)}]_{z=0}$	0.218	1.147	0.689	0.536
$\epsilon_2(\overline{u^2\theta_z})_{z=0}$	0.216	1.351	0.820	0.555

TABLE 3: Comparison of the different contributions to the Nusselt number, and some approximations of these.

In figure 3 some dispersion effects on the temperature field are shown. The isotherms may be significantly distorted. The solid curves are isotherms for the case  $D = 1/150$ , while the dashed curves are corresponding isotherms for  $D = 0$ . The effects increase strongly with increasing Rayleigh numbers. It is interesting to study the vicinity of the lower boundary: In the region of up-going fluid the temperature gradient is reduced by dispersion. In most of the region of down-going fluid the gradient is steepened. The former effect is always the stronger, so that the average temperature gradient is reduced due to dispersion.

The streamline pattern is never distorted significantly by dispersion in our range of computation. The velocity amplitude however, is influenced by dispersion. Following Palm, Weber and Kvernfold (1972), the root mean square velocity of a cell is approximately given by

$$\overline{(\vec{v}^2)}^{\frac{1}{2}} = Ra^{\frac{1}{2}}(Nu-1)^{\frac{1}{2}} \quad (4.2)$$

where the pointed bracket denotes vertical average. By means of (2.8), this enables us to estimate the average Péclet number defined by

$$Pe^{(ave)} = \overline{(\vec{v}^2)}^{\frac{1}{2}} \frac{\kappa_m}{\kappa_f} \frac{d}{h} = Re^{\frac{1}{2}}(Nu-1)^{\frac{1}{2}} \frac{\kappa_m}{\kappa_f} \frac{d}{h} \quad (4.3)$$

Deviations from our theory become significant when  $Pe^{(ave)}$  is about 10. We notice that  $Pe^{(ave)}$  cannot be expressed by  $D$  alone, so that formula (4.3) must be applied to each specific case.

We have investigated the stability of this steady nonlinear roll solution in the case of  $D = 1/150$ . The results are displayed in figure 4, and compared with the case of  $D = 0$ . The zig-zag instability is not significantly influenced by dispersion. The rest of the stability domain is bounded by cross-roll disturbances, which may be strongly influenced by dispersion.

At moderately supercritical Rayleigh numbers ( $Re < 5 Ra_c$ ), dispersion slightly reduces the range of stable wave numbers. However, at larger Rayleigh number a strong extension of the stability domain is present. The second critical Rayleigh number, above which no stable steady solution exists, is drastically delayed. Actually, our choice  $D = 1/150$  is not small enough to determine this upper limit, within our range of computation.

## 5. COMPARISON WITH EXPERIMENTS

In this chapter the results from the analysis above will be compared with some experimental data of the heat transport. In figure 5 some data from Buretta (1972) are shown. This experimental series was performed with glass beads saturated by water, where  $\kappa_m/\kappa_f = 3.75$  and  $d/h = 1/15$ . The corresponding value of the dispersion factor is  $1/60$ . Our theoretical curve for  $D = 1/60$  shows excellent agreement with Buretta's experiments. For comparison the theoretical curve for neglect of dispersion is displayed. This clearly demonstrates the importance of dispersion.

From formula (4.3) the average Péclet number at the termination of our theoretical curve in figure 5 is about 15. Then our theory may be inappropriate. Only up to  $Ra$  about 200 - 300 the conditions of our theory are fulfilled. The average Reynolds number does not exceed 2.

In figure 6 two sets of experimental data by Combarnous (1970) are compared with the present theory. Also these experiments are performed with glass beads in water. It is interesting that the theoretical trend of increased heat transport for increased coarseness of the porous medium is actually confirmed by these experiments. The upper and lower theoretical curve corresponds to  $D = 1/60$  and  $D = 1/107$ , respectively. We have chosen to terminate these curves at Péclet numbers of 15 and 10, respectively, and Reynolds numbers less than 2.

The experimental data of figures 5 and 6 indicate an inflexion point in the Nusselt number curves. This phenomenon was explained by Combarnous (1970) by the occurrence of a new linearly unstable mode. However, such a point of view lacks foundation within nonlinear theory.



The present theory gives an alternative explanation which seems very good. One must, however, keep in mind that these effects become important at Péclet numbers not far below the value at which our approximations become uncertain.

There are many other experiments confirming the trend of our theory giving a Nusselt number above the value of ordinary porous convection. See the review article by Cheng (1978). It is, however, desirable to perform experiments with a systematic variation of the dispersion factor,  $D$ . Most experiments involve a ratio  $d/h$  not small enough for dispersion effects to be neglected. Experiments on more finely grained media are wanted. They are hoped to give a closer approximation to the theory of ordinary porous convection (Straus 1974).

When the pore Reynolds number exceeds unity, the flow resistance is higher than predicted by Darcy's linear law, due to a nonlinear friction term (see Bear 1972, p. 126). In this regime the velocity amplitude is smaller than predicted by our theory. This will cause a considerable reduction in the heat transport, which is observed in the experiments by Schneider (1963) and Elder (1967). Heat dispersion will be strongly reduced, as it is a quadratic function of velocity.

The effect of dispersion compared with the nonlinear term in Darcy's law is indicated by the Prandtl number of the fluid

$$\text{Pr} = v/\kappa_f \quad (5.1)$$

In the present study we have assumed that dispersion is more important than the nonlinear term in Darcy's law, which means that  $\text{Pr} > 1$ .

6. SUMMARY

The influence of hydrodynamic dispersion on thermal convection in a porous layer has been investigated theoretically. The steady, supercritical motion, the heat transport and the stability of the motion have been examined.

The magnitude of the dispersion effects is characterized by the dispersion factor  $D = (\kappa_m/\kappa_f)(d/h)^2$ , depending strongly on the coarseness of the porous material. Hydrodynamic dispersion slightly reduces the heat transport when  $Ra < 1.63 Ra_c$ , but increases it with rapidly growing strength when the Rayleigh number increases further. Hydrodynamic dispersion strongly extends the range of Rayleigh numbers giving stable convection rolls.

The present theory should be useful at average Péclet numbers smaller than 10 and average Reynolds numbers not above the order of 1. Our theoretical predictions of the heat transport show good agreement with experimental data by Buretta (1972) and Combarous (1970). This accordance lends support to the dispersion theory by Saffman (1960) on which this study is based.

REFERENCES

- Bear, J. 1969 Hydrodynamic Dispersion. In: R.de Wiest (Editor), Flow through Porous Media, Academic Press.
- Bear, J. 1972 Dynamics of Fluids in Porous Media. Elsevier.
- Buretta, R. 1972 Ph.D. dissertation, University of Minnesota.
- Cheng, P. 1978 Adv. Heat Transfer 14, 1.
- Combarous, M. 1970 Thèses de Dr. ès Sc. Phys., Univ. de Paris.
- Combarous, M.A. & Bories, S.A. 1975 Adv. Hydrosoc. 10, 232.
- Elder, J.W. 1967 J. Fluid Mech. 27, 29.
- Fried, J.J. 1975 Groundwater Pollution, Elsevier.
- Fried, J.J. & Combarous, M.A. 1971 Adv. Hydrosoc. 7, 169.
- Green, D.W. 1963 Ph.D. dissertation, Univ. of Oklahoma
- Horton, C.W. & Rogers, F.T. 1945 J. Appl. Phys. 16, 367.
- Kuo, H.L. 1961 J. Fluid Mech. 10, 611.
- Kvernfold, O. 1975 Univ. Oslo Preprint Ser. no. 1.
- Neischloss, H. & Dagan, G. 1975 Phys. Fluids, 18, 757.
- Palm, E., Weber, J.E. & Kvernfold, O. 1972 J. Fluid Mech. 54, 153.
- Pfannkuch, H.O. 1963 Rev. Inst. Fr. Pétr. 18, 215.

- Poreh, M. 1965 J. Geophys. Res. 70, 3909.
- Rubin, H. 1974 J. Hydrol. 21, 173.
- Saffman, P.G. 1959 J.Fluid Mech. 6, 321.
- Saffman, P.G. 1960 J.Fluid Mech. 7, 194.
- Schlüter, A., Lortz, D. & Busse, F. 1965 J.Fluid Mech. 23, 129.
- Schneider, K.J. 1963 11th Int.Cong. of Refrigeration, Munich  
Paper, no. 11-4.
- Straus, J.M. 1974 J.Fluid Mech. 64, 51.
- Taylor, G.I. 1953 Proc. Roy.Soc. (London) A 219, 186.
- Tyvand, P.A. 1977 J. Hydrol. 34, 335.
- Weber, J.E. 1975 J. Hydrol. 25, 59.

FIGURE LEGENDS

- Fig. 1        Nu vs.  $Ra/Ra_c$  for some values of  $D = (\kappa_m/\kappa_f)(d/h)^2$ .
- Fig. 2        Nu vs.  $\alpha/\pi$  for some values of  
 $Ra/Ra_c$ . —,  $D = 1/80$ . ---,  $D = 0$ .
- Fig. 3        Isotherms for  $T - \frac{\Delta T}{T_0}$ . —,  $D = 1/150$ . ---,  $D = 0$ .  
(a)  $R/R_c = 4$ . (b)  $R/R_c = 6$ .
- Fig. 4        Stability domains for the steady two-dimensional  
motion in the  $\alpha/\alpha_c, R/R_c$  plane. —, cross-roll  
instability. —x—, zig-zag instability.
- Fig. 5        Nu vs. Ra. —, theoretical curves. •, expe-  
riments by Buretta (1972).
- Fig. 6        Nu vs. Ra. —, theoretical curves. Upper curve,  
 $D = 1/60$ . Lower curve,  $D = 1/107$ . •, experiments  
by Combarous (1970), with  $d/h = 1/15$ ,  
 $\kappa_m/\kappa_f = 3.75$ . + experiments by Combarous (1970),  
with  $d/h = 1/20$ ,  $\kappa_m/\kappa_f = 3.75$ .

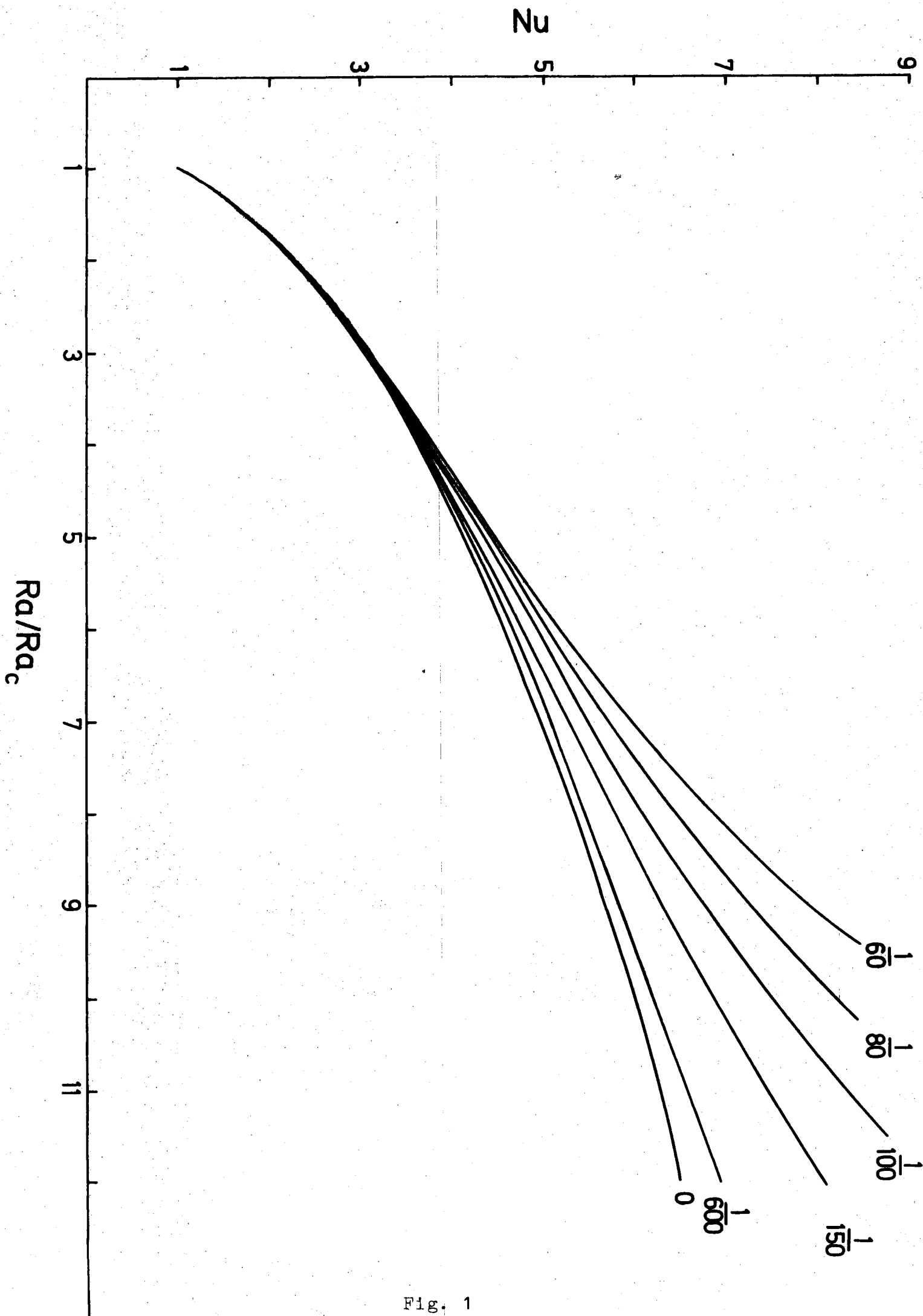


Fig. 1

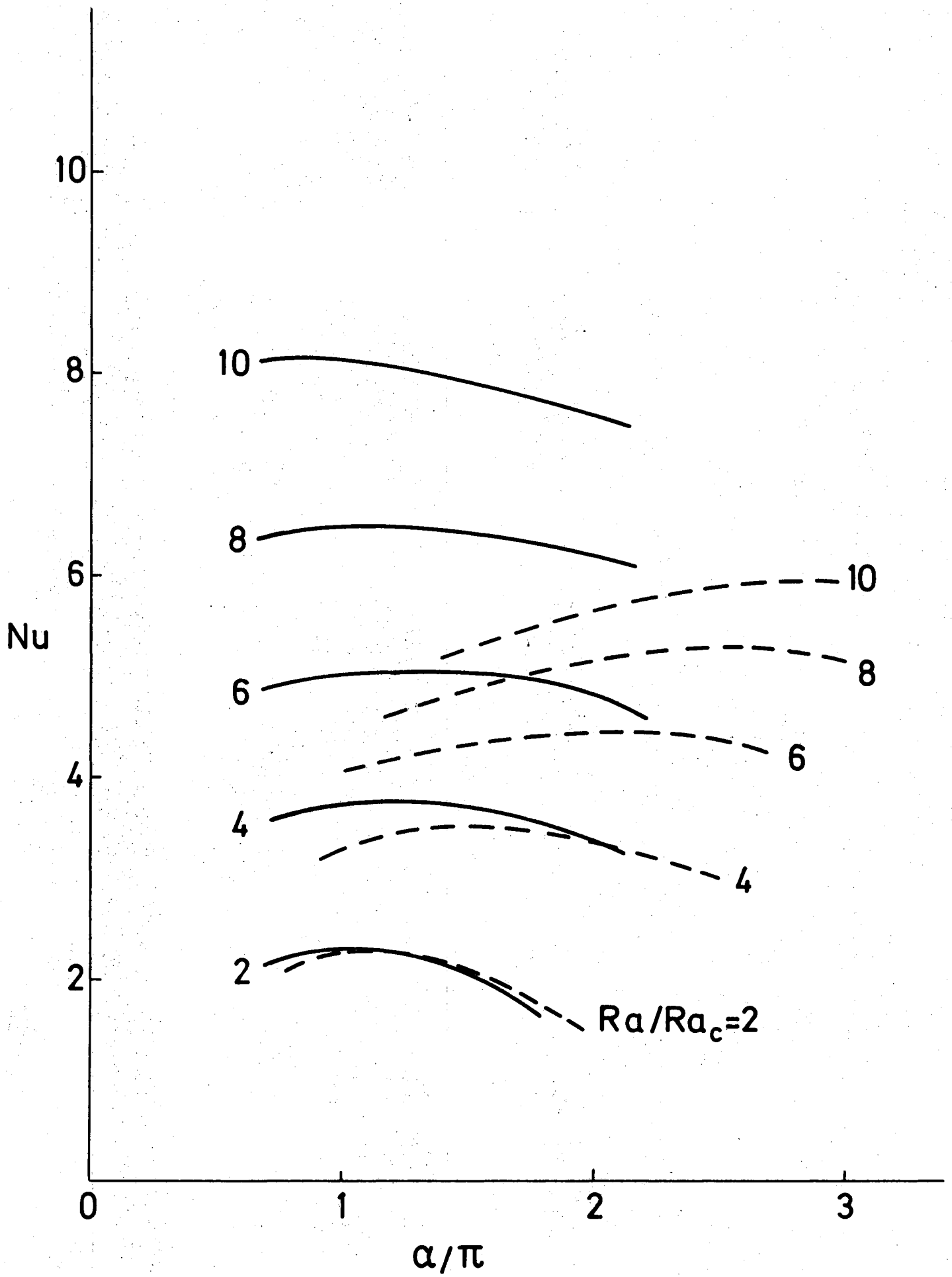


Fig. 2

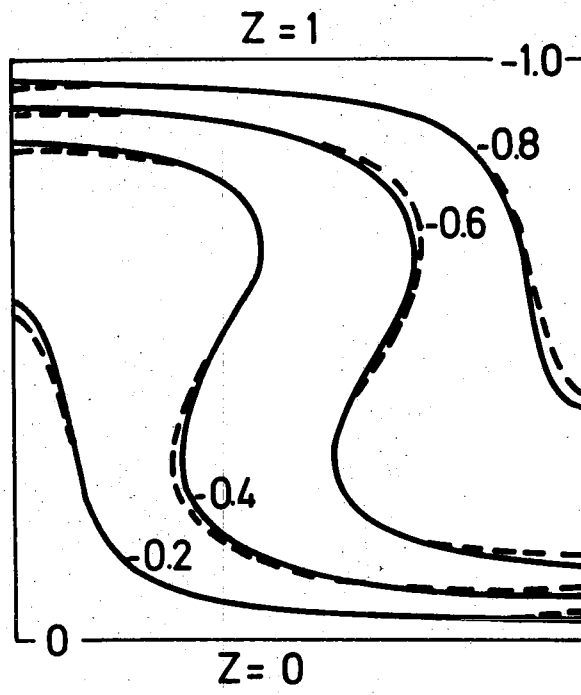


Fig. 3 (a)

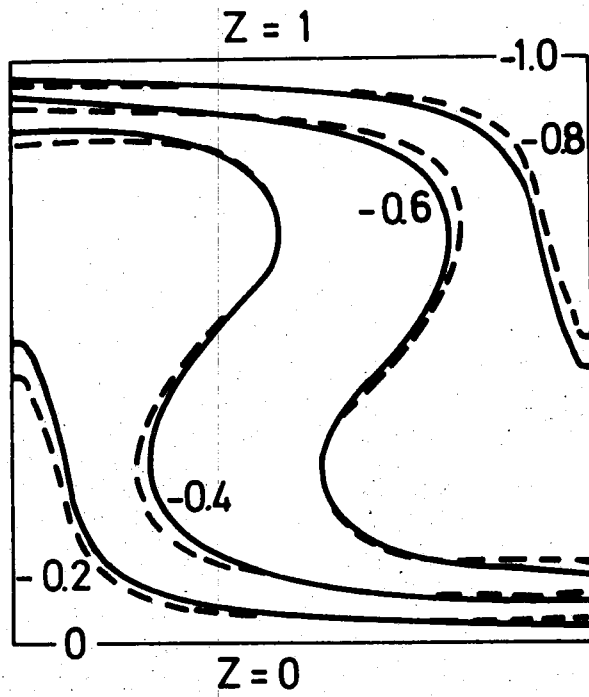


Fig. 3 (b)



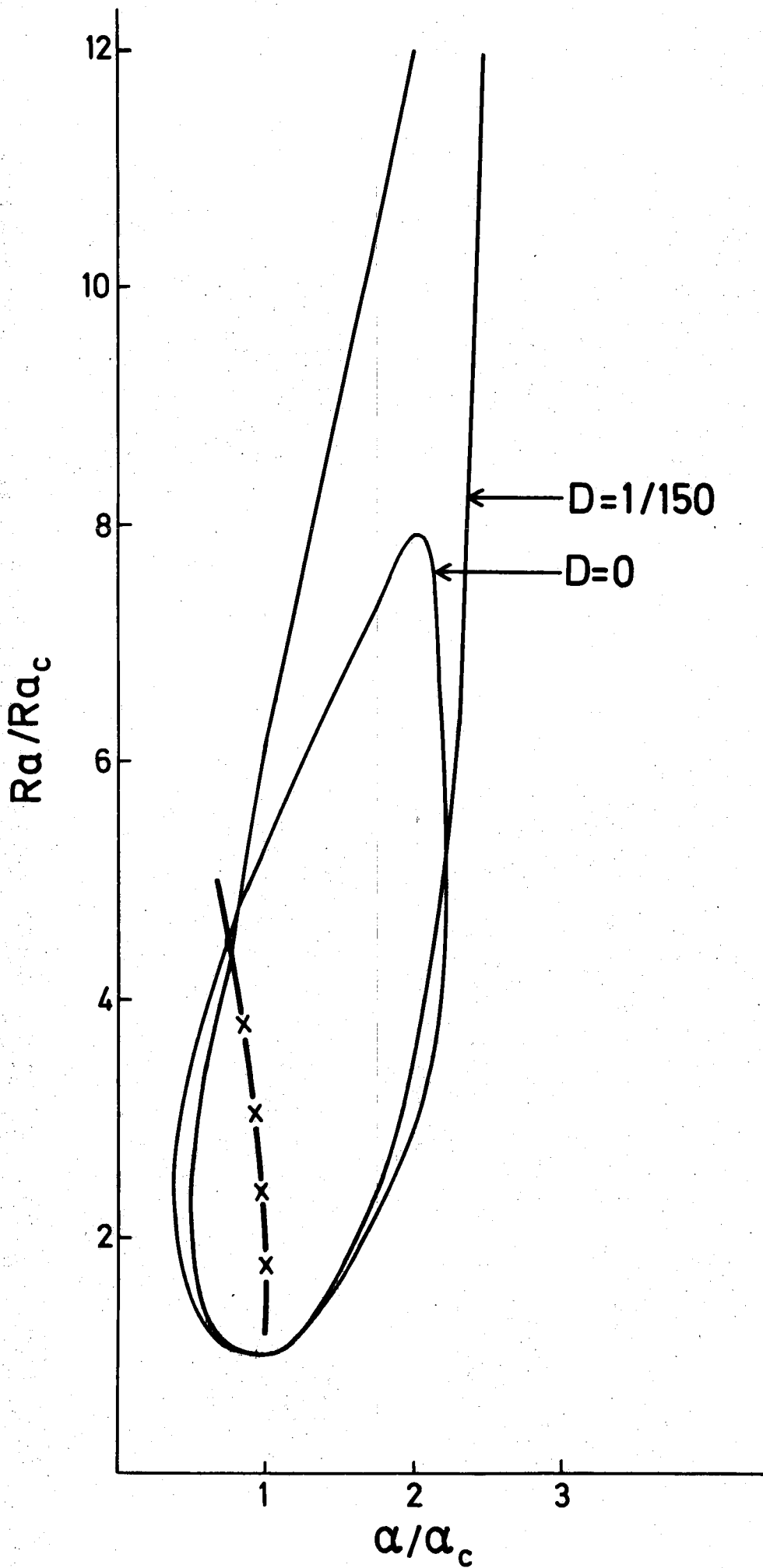


Fig. 4

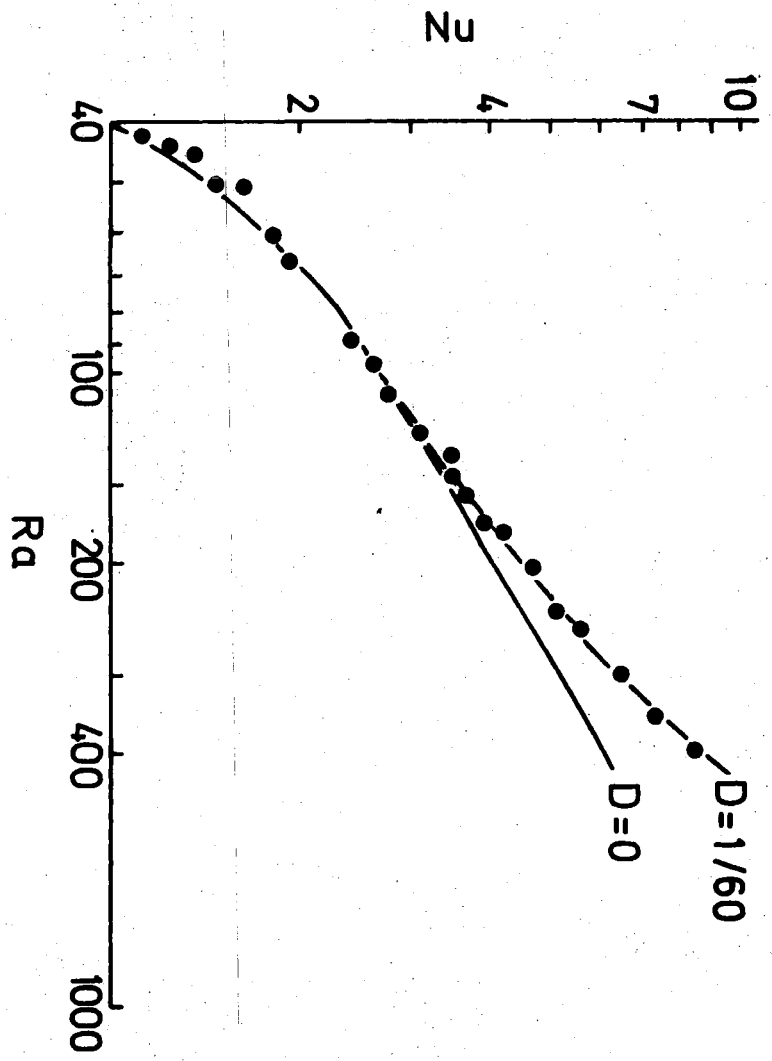


Fig. 5

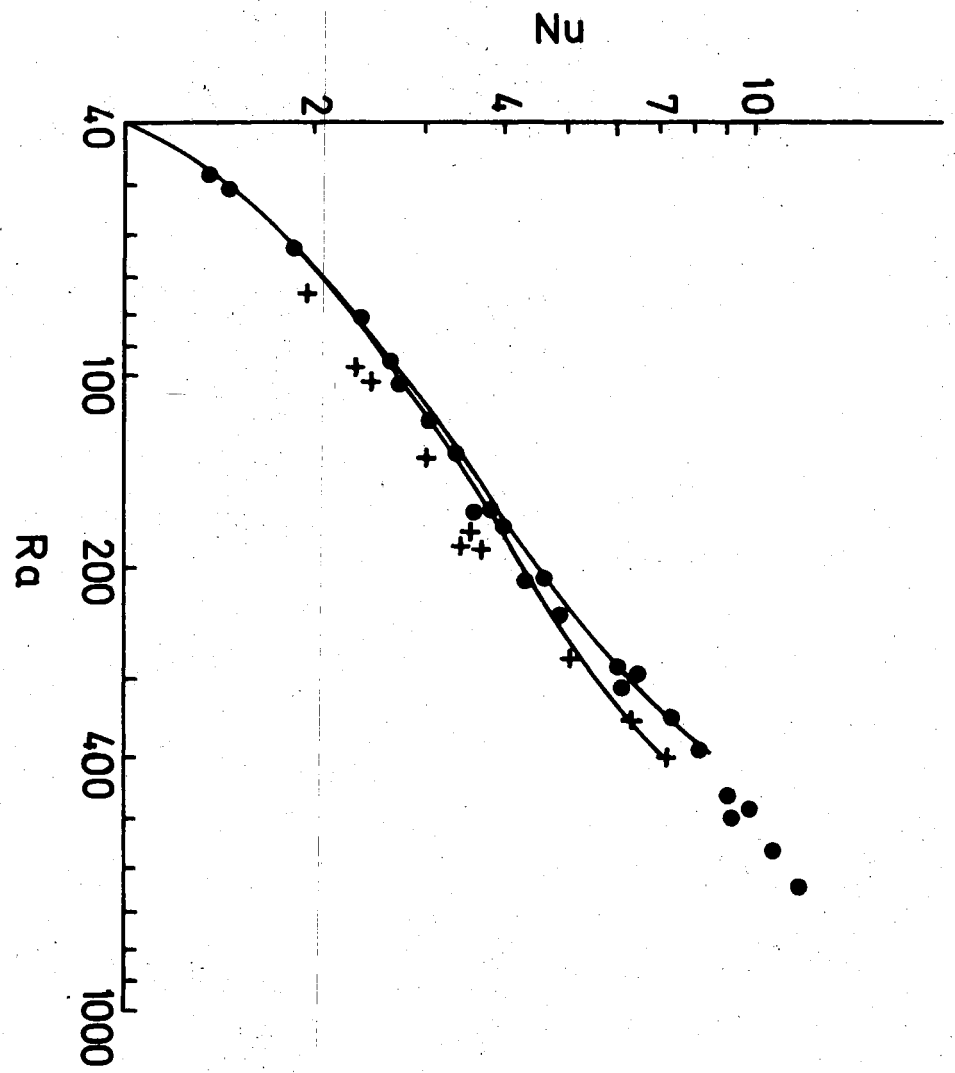


Fig. 6